Journal of Chromatography A, 1218 (2011) 1828–1834

Contents lists available at ScienceDirect

Journal of Chromatography A

journal homepage: www.elsevier.com/locate/chroma

Binding behaviour of molecularly imprinted polymers prepared by a hierarchical approach in mesoporous silica beads of varying porosity

Claudio Baggiani *, Patrizia Baravalle, Cristina Giovannoli, Laura Anfossi, Cinzia Passini, Gianfranco Giraudi

Laboratory of Bioanalytical Chemistry, Department of Analytical Chemistry, University of Torino, via Giuria 5, 10125 Torino, Italy

ARTICLE INFO

Article history:
Received 6 October 2010
Received in revised form
28 December 2010
Accepted 2 February 2011
Available online 23 February 2011

Keywords:
Molecular imprinting
Silica beads
Bulk polymerization
Non linear chromatography
Peak profiling
Affinity constant
Binding site concentration
Rate constant

ABSTRACT

One of the most interesting methods for preparing molecularly imprinted polymers with controlled morphology consists in filling the pores of silica beads with an imprinting mixture, polymerizing it and dissolving the support, leaving porous imprinted beads that are the "negative image" of the silica beads. The main advantage of such an approach consists in the easy preparation of spherical imprinted polymeric particles with narrow diameter and pore size distribution, particularly indicated for chromatographic applications. In this approach it has been shown that the resulting morphology of polymeric beads depends essentially on the porosity and surface properties of the silica beads that act as microreactors for the thermopolymerization process. Anyway, it is not yet clear if the porosity of the silica beads influences the binding properties of the resulting imprinted beads. In this paper, we report the effect of different porosities of the starting mesoporous silica beads on the resulting binding properties of imprinted polymers with molecular recognition properties towards the fungicide carbendazim. The morphological properties of the imprinted beads prepared through this hierarchical approach were measured by nitrogen adsorption porosimetry and compared with a reference imprinted material prepared by bulk polymerization. The chromatographic behaviour of HPLC columns packed with the imprinted materials were examined by eluting increasing amounts of carbendazim and extracting the binding parameters through a peak profiling approach. The experimental results obtained show that the resulting binding properties of the imprinted beads are strongly affected by the polymerization approach used but not by the initial porosity of the silica beads, with the sole exception of the binding site density, which appears to be inversely proportional to them.

© 2011 Elsevier B.V. All rights reserved.

1. Introduction

The most popular method for obtaining molecularly imprinted polymers (MIPs) consists of a bulk polymerization which produces a monolithic material that has to be crushed and sieved to obtain particles of the desired size distribution [1]. Despite being a convenient approach, it shows many drawbacks. First of all, the sieved material is highly irregular, without an effective possibility to obtain homogeneous fractions. This fact dramatically reduces the chromatographic efficiency of a column packed with such a material. The procedure of grinding and sieving is cumbersome, and it causes a significant loss of polymer. Moreover, most of the lost material consists of sub-micrometric powders, which could adhere to the bigger particles and cause excessively high back-pressures in a chromatographic column during and after the packing procedure when multiple washings and careful sedimentation of the polymer are not performed. Again, for its strongly exothermal nature, bulk polymerization cannot be safely scaled-up without the risk of dangerous overheating of the polymerization vessel. Finally, the greater part of the imprinted binding sites are often located deep in the bulk of the polymer, raising an issue of poor accessibility and slow diffusion kinetics, which represents a significant problem in the chromatographic applications of MIPs.

With the purpose of overcoming the drawbacks of bulk polymerization, several alternative approaches based on the synthesis of imprinted beads have been proposed in recent years [2–4]. One of the most interesting methods consists of filling the pores of silica beads with an imprinting mixture, polymerizing it and dissolving the support, leaving porous imprinted beads that are the "negative image" of the silica beads. This hierarchical approach was proposed for the first time by Yilmaz et al. [5]. In this work, theofilline was covalently immobilized in the pores of aminated silica beads through the use of a spacer arm. Then, an imprinting mixture was used to fill the pores of the beads. After the end of the polymerization process, the silica support was etched away, leaving imprinted binding sites on the surface of the remaining polymeric

* Corresponding author. Tel.: +39 0116707846; fax: +39 0116707615.
E-mail address: claudio.baggiani@unito.it (C. Baggiani).

0021-9673/$ – see front matter © 2011 Elsevier B.V. All rights reserved.
doi:10.1016/j.chroma.2011.02.003

beads. The main advantage of such an approach consists of the easy preparation of spherical imprinted polymeric particles of narrow diameter and pore size distribution, particularly indicated for chromatographic applications. The validity of this approach was further demonstrated for imprinted beads with molecular recognition properties towards 9-ethyladenine and triaminopyrimidine [6], the protected dipeptide FMOC-PheGly-OH [7,8] and bisphenol A [9]. In a simpler approach, isoproterenol-imprinted beads were prepared by filling pores of butyl-capped silica beads with a polymerization mixture containing the template, thus eliminating the need for the covalent immobilization of the template on the surface of the silica pores [10]. This method was confirmed by Tamayo et al. [11,12], who successfully used porous beads composed of bare silica to prepare propazine- and linuron-imprinted polymeric beads, and used them for direct chromatographic screening of phenylurea herbicides in vegetable samples.

In this approach it has been shown that the resulting morphology of polymeric beads depends essentially on the porosity and surface properties of the silica beads that act as microreactors for the thermopolymerization process. Anyway, it is not yet clear how the porosity of the silica beads influences the binding properties of the resulting imprinted beads.

In this paper, we describe the effect of different porosities of the starting mesoporous silica beads on the resulting binding properties of imprinted polymers with molecular recognition properties towards the fungicide carbendazim. The morphological properties of these imprinted beads were measured by nitrogen adsorption porosimetry and compared with a reference imprinted material prepared by bulk polymerization. The chromatographic behaviour of HPLC columns packed with the imprinted materials were examined by eluting increasing amounts of carbendazim and extracting the binding parameters through a peak profiling approach.

2. Experimental

2.1. Materials

Benomyl was from Dr. Ehrenstorfen GmbH (Augsburg, Germany). Ammonium hydrogen fluoride, 2,2′-azo-bis-(2-methylpropionitrile), carbendazim, ethylene dimethacrylate, hexamethyldisilazane, methacrylic acid and 35-45 μm spherical silica gel beads (S1, Fluka cat.num.95021; S2, Fluka cat.num.86981; S3, Fluka cat.num.89752) were from Sigma–Aldrich–Fluka (Milan, Italy). Acetic acid, acetone, acetonitrile, chloroform, ethanol and toluene were from VWR International (Milan, Italy).

Chloroform was distilled before use to eliminate the stabilizer (ethanol). Polymerization inhibitors in vinyl monomers were removed by cleanup on activated alumina columns. Carbendazim stock solutions were prepared by dissolving 50.0 mg of substance in 5.00 ml of acetonitrile and stored in the dark at −20 °C. All the solvents were of HPLC quality, other chemicals were of analytical grade.

The high-performance liquid chromatography apparatus (L-6200 constant-flow binary pump, L-4250 UV–Vis detector, Rheodyne 7100 six-port injection valve provided with 5 μl injection loop and a D7000 data acquisition system) was from Merck-Hitachi (Darmstadt, Germany).

2.2. Synthesis of molecularly imprinted beads

In a 500 ml round-bottomed flask, 5.0 g of silica gel beads were suspended in 50 ml of 6 M hydrogen chloride aqueous solution under sonication. The homogenous dispersion was refluxed overnight, diluted with 450 ml of cold ultrapure water and filtered on a nylon membrane (0.22 μm nominal porosity). The beads were washed with ultrapure water till neutrality, transferred in a 500 ml round-bottomed flask and dried at 105 °C overnight. The dried silica beads were transferred in a 250 ml round-bottomed flask and dispersed in 100 ml of toluene, removing water by azeotropic distillation. Then, the flask was cooled to room temperature, 810 μl of hexamethyldisilazane (5 mmoles) were added and the mixture gently stirred overnight. The silanized silica glass beads were filtered on a nylon membrane (0.22 μm nominal porosity), washed with acetone, dried under vacuum and stored in a dessicator at room temperature.

The prepolymerization solution was prepared in a 50 ml Erlenmayer flask by mixing 3 mmoles of benomyl, 9 mmoles of methacrylic acid, 81 mmoles of ethylene dimethacrylate and 200 mg of 2,2′-azo-bis-(2-methylpropionitrile) into 17 ml of dried chloroform. Then, the mixture was purged with nitrogen and sonicated in a water bath for 5 min.

In order to obtain discrete silica–polymer composite beads and to prevent particle agglomeration the amount of prepolymerization mixture added to the silica beads was slightly lower (about 5%) than the nominal pore volume of the silica. Thus, in 10 ml thick wall glass vials maintained under continuous sonication to remove any entrapped air bubbles, adequate amounts of the prepolymerization mixture were slowly added to 3 g of silica beads. Then, mixtures were homogenized with a steel spatula obtaining free-flowing powders, sparged with a gentle stream of nitrogen, sealed and allowed to polymerize in a water bath at 65 °C for 3 days.

After polymerization was completed, the silica–polymer composites were transferred into screw-capped polypropylene tubes and 10 ml of acetone were added to increase the wettability of the beads. Then 20 ml of 3 M ammonium hydrogen fluoride aqueous solution was added. Suspensions were gently stirred overnight to completely dissolve the silica matrix of the composites. After dissolution of the silica, suspensions of imprinted polymeric beads (namely, MIP-S1, MIP-S2 and MIP-S3) were diluted with 100 ml deionised water, filtered on a polycarbonate filter funnel equipped with a nylon membrane (0.22 μm nominal porosity) and washed extensively with deionised water till neutrality.

A molecularly imprinted bulk polymer (MIP-B) was prepared from the same prepolymerization mixture as previously described [13]. The polymer obtained was broken, mechanically ground, and wet-sieved to 35–50 μm particle size.

2.3. Nitrogen sorption measurements

Nitrogen adsorption/desorption isotherms were measured at 77.2 K on an porosimetry analyzer ASAP 2020 (Micromeritics Instruments Corporation, Norcross, GA, USA).

Before measurements, 100–150 mg of the samples were degassed by heating at 378 K under high vacuum (10^{-5} Pa) for 3 h. The specific mesopore surface area (S) was calculated in the p/p_0 range of 0.05–0.30 of the nitrogen adsorption isotherm using the BET theory [14]. The volume of mesopores in the range 2–50 nm (V_p) was calculated from the amount of nitrogen vapor adsorbed at a relative pressure close to unity, on the assumption that all the pores are filled with liquid nitrogen. The average mesopore diameter (d_p) was calculated as $d_p = 4V_p/S$, assuming cylindrical geometry.

2.4. Column packing

Adequate amount of polymers were suspended in a 1 + 1 (v/v) ethanol–water mixture, and the slurry was packed in 3.9 × 100 mm (V_{col} = 1.194 cm^3) stainless-steel HPLC columns. The packing of the stationary phases was performed by gradually adding the slurry of the polymer to the column and eluting it with 1 + 1 (v/v) ethanol–water mobile phase at constant pressure of 15 MPa. The packed columns were washed at 1 ml/min with 9 + 1 (v/v)

ethanol–acetic acid until a stable baseline was reached (294 nm). After equilibration, the pressure in the columns was 6 MPa using acetonitrile–acetic acid 99 + 1 (v/v) as a mobile phase and at a flow rate of 1 ml/min.

2.5. Liquid chromatography

Columns were equilibrated with 99 + 1 (v/v) acetonitrile–acetic acid at a flow rate of 1.0 ml/min for 30 min. Then, 5 μl of 99 + 1 (v/v) acetonitrile–acetic acid solutions of carbendazim were injected and eluted at 1.0 ml/min, and the absorbance recorded at 294 nm. The concentrations used in this study were: 2, 5, 7.5, 10, 25, 50, 75, 100, 250, 500, 750, 1000 and 2000 μg/ml. Each elution was repeated three times to assure chromatogram reproducibility. At the end of each run, the column was flushed with the mobile phase for 30 min. Column void volumes (t_0, 0.98 ml for MIP-S1, 1.01 ml for MIP-S2 and MIP-S3, and 0.99 ml for MIP-B) were measured by eluting 5 μl of acetone 0.1% (v/v) in 99 + 1 (v/v) acetonitrile–acetic acid, and the absorbance recorded at 270 nm.

The averaged experimental chromatograms were smoothed by using a Savitzky–Golay filter, normalized for the column void volume ($t = t - t_0$), and analyzed using the non-linear chromatography (NLC) model derived from impulse input solution [15] and described as follows:

$$s(t) = \frac{m_0}{m_3}\left(1 - \exp\left(\frac{m_3}{m_2}\right)\right) \times \left(\frac{\sqrt{m_1/t}\left(2\sqrt{m_1 t}/m_2\right)\exp\left(-(t+m_1)/m_2\right)}{1 - T\left(m_1/m_2, t/m_2\right)\left(1 - \exp\left(-(m_3/m_2)\right)\right)}\right) \quad (1)$$

$$T(u, v) = \exp(-v)\int_0^u \exp(-t) I_0 2\sqrt{vt}\, dt$$

where $s(t)$ is the peak height at time t, I_n the modified Bessel function of nth-order, $m_0 - m_3$ the peak's parameters corresponding, respectively, to the peak area (area, m_0), the retention time measured at the centre of gravity of the peak (centre, m_1), the peak variance (width, m_2) and the peak skew (distortion, m_3). The $T(u, v)$ function is a "switching" function, which causes the skew in the peak profile when the column is overloaded.

The filtered data was processed using the NLC function routine reported in PeakFit 4.11 for Windows software (Systat Software Inc., Richmond, CA, USA). To assure robust results, Pearson VII limit minimization was chosen as the minimization method. To avoid being trapped in local minima, which give incorrect results, the fitting was carried out several times using different initial guess values for the parameters $m_0 - m_3$. The NLC parameters were further processed for the calculation of the retention time measured at the centre of gravity of the peak (k), the apparent affinity constant (K) and binding site density (Λ_0), the lumped kinetic association (k_a) and dissociation (k_d) rate constants values. These parameters were calculated using the following relationships [15,16]:

$$k = m_1 \quad (2)$$

$$K = \frac{m_3}{C_0} \quad (3)$$

$$k_a = \frac{m_1}{m_2 t_0} \quad (4)$$

$$k_d = \frac{1}{m_2 t_0} \quad (5)$$

$$\Lambda_0 = \frac{\varepsilon}{\rho S}\frac{k}{K} \quad (6)$$

where C_0 is the solute molar concentration multiplied by the width of the injection pulse (expressed as fraction of column void volume), ε the column porosity ratio, ρ the density of the stationary phase and S is the specific surface.

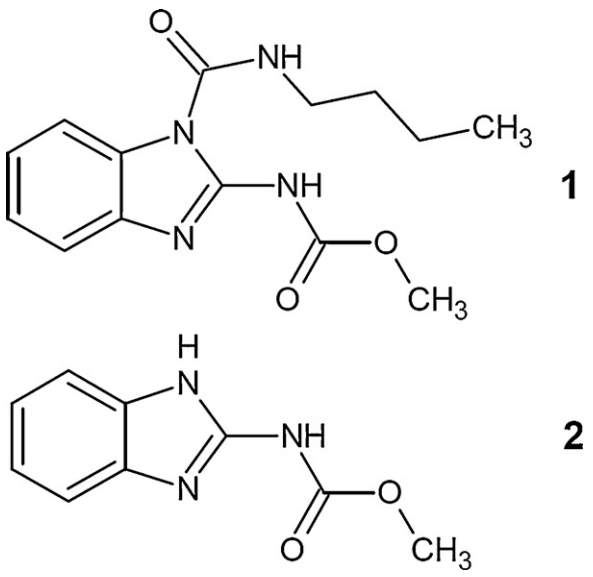

Fig. 1. Molecular structures of benomyl (methyl-1-(butylcarbamoyl)benzimidazol-2-ylcarbamate, **1**) and carbendazim (methylbenzimidazol-2-ylcarbamate, **2**).

3. Results and discussion

In this work we focused our attention on molecularly imprinted beads with recognition properties towards the fungicide carbendazim. These beads were prepared by an hierarchical approach, using three commercial silica beads of different porosities as a support. The pre-polymerization mixture was designed in accordance with our previous work, where benomyl (methyl-1-(butylcarbamoyl)-benzimidazol-2-ylcarbamate, Fig. 1, **1**) was used to successfully prepare an imprinted polymer with excellent binding properties towards the related molecule carbendazim (methylbenzimidazol-2-ylcarbamate, Fig. 1, **2**) [13]. After the imprinting step, the dissolution of the silica support through the use of an ammonium fluoride concentrated solution (about 3 M) left free-flowing polymeric beads, without any aggregates visible to the naked eye. This indicates that no polymerization occurred outside of the porous silica beads.

3.1. Nitrogen sorption measurements

As stated in Section 1, although the imprinted binding sites are responsible for the binding properties towards the template molecule and its analogues, the morphology of the imprinted polymer also can have an effect, especially determining the amount of accessible binding sites through its porosity. Thus, pore volume, pore size and surface area should influence the separation performance of a molecularly imprinted stationary phase. As a consequence, to correctly compare the chromatographic binding properties (apparent affinity constant (K), binding site density (Λ_0), lumped kinetic association (k_a) and dissociation (k_d) rate constants) of the different particle types, we measured beads porosity in the mesopore range by nitrogen adsorption at 77 K.

Fig. 2 shows the nitrogen adsorption isotherms of the beads (MIP-S1, MIP-S2 and MIP-S3) and of the bulk particles (MIP-B). All the polymers prepared from mesoporous silica beads exhibit clear Brunaurer's Type IV isotherms, relative to predominant mesoporosity. On the contrary, bulk particles exhibit a different isotherm, with a very limited hysteresis loop in the adsorption–desorption

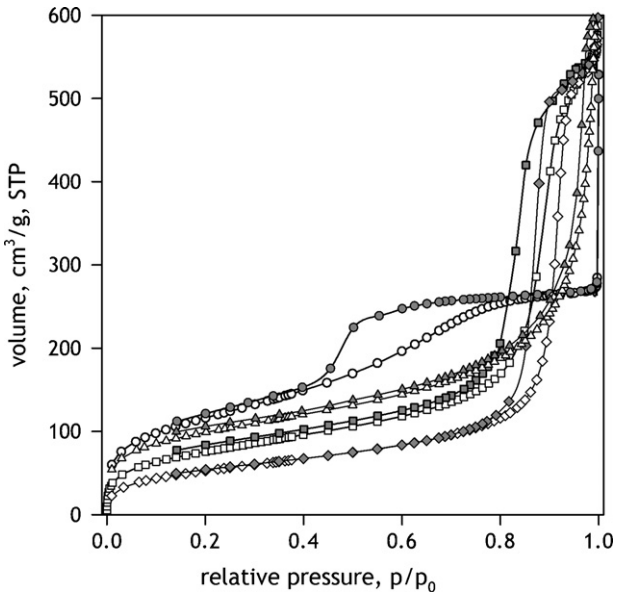

Fig. 2. Low temperature (77 K) nitrogen adsorption (open symbols) and desorption (gray symbols) isotherms for MIP-S1 (circles), MIP-S2 (squares), MIP-S3 (diamonds) and MIP-B (triangles).

process. This isotherm can be identified with a material where macroporosity predominates on mesoporosity. This distribution is confirmed by the calculated differential pore distributions in the 1.7–300 nm range, reported in Fig. 3, where it is possible to see that silica-derived beads show a mean porosity increasing in the order MIP-S3 > MIP-S2 > MIP-S1 but well below that of the bulk material MIP-B. Notwithstanding, the silica-derived beads clearly show a narrower pore size distribution compared to the bulk material, that is characterized by a very broad pore size distribution with a mean porosity shifted towards the macroporosity range (>50 nm), typical of this kind of polymers.

Comparing the mesoporosity parameters reported in Table 1, it is clear that the synthesis of imprinted materials in the pores of preformed silica beads produces beads with decreased mesopore diameter and volume, and increased surface area respect to the starting silica beads.

Table 1
Specific surface area (S), volume of mesopores in the range 2–50 nm (V_p) and average mesopore diameter (d_p) measured for silica beads, imprinted beads and bulk particles.

	S ($m^2\ g^{-1}$)	V_p ($cm^3\ g^{-1}$)	d_p (nm)
S1[a]	300	0.85	10
MIP-S1	403	0.680	6.7
S2[a]	210	0.80	20
MIP-S2	262	0.796	12.2
S3[a]	100	0.80	30
MIP-S3	183	0.822	18.0
MIP-B	334	0.833	10.0

[a] Mean values declared by manufacturer.

3.2. Binding properties

As previously reported by several authors, the non-linear chromatographic theory can offer important insights on the binding behaviour – both in terms of thermodynamic and kinetic parameters – of molecularly imprinted polymers packed in chromatographic columns [16–21]. Particularly, Toth was the first to use NLC to investigate silica beads filled with molecularly imprinted polymers [20].

In our approach, peak profiles corresponding to increasing amounts of carbendazim were recorded (an example is reported in Fig. 4) and analyzed using the NLC equation, which resulting parameters m_1–m_3 were determined for each concentration of solute. The centre of mass of a chromatographic peak – defined in the NLC model by the parameter m_1 of Eq. (1) – corresponds to the thermodynamic capacity factor, that is of the very analyte used in the experimental conditions considered without any contribution caused by kinetic effects. Thus, when overloading effects become significant, non-linearity could clearly be observed as a drift of parameter m_1 towards low values, corresponding to a net loss of column capacity proportional to the amount of analyte injected. On the contrary, when overloading effects can be neglected, the "thermodynamic" capacity factor becomes nearly

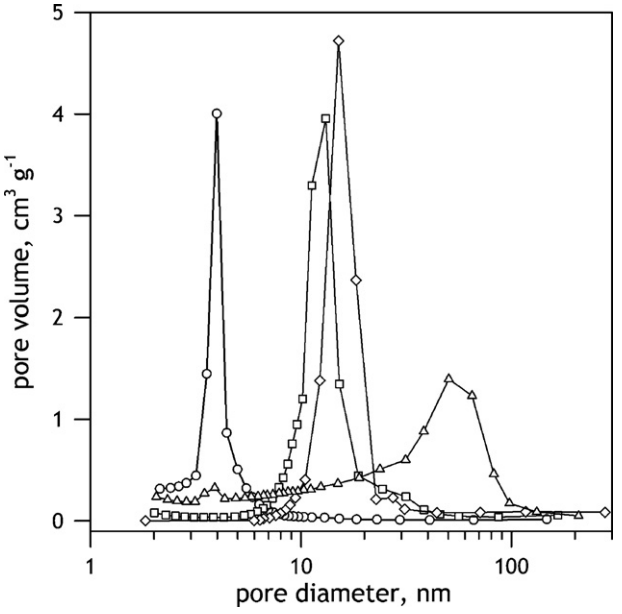

Fig. 3. Pore size distribution in the 1.4–300 nm range computed from the desorption branch of the isotherm by the BJH method for MIP-S1 (circles), MIP-S2 (squares), MIP-S3 (diamonds) and MIP-B (triangles).

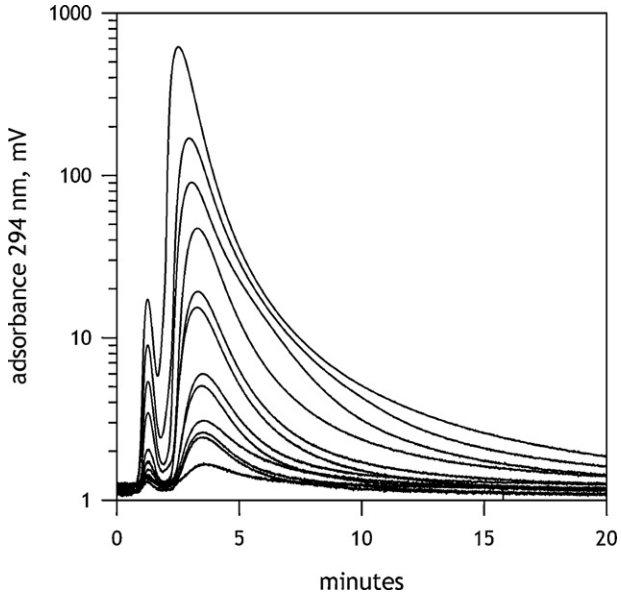

Fig. 4. Elution of increasing amount of carbendazim in the range 10 ng–10 μg (injections of 5 μl of carbendazim solutions in the concentration range of 2–2000 μg/ml) on the column packed with polymer MIP-S3P1.

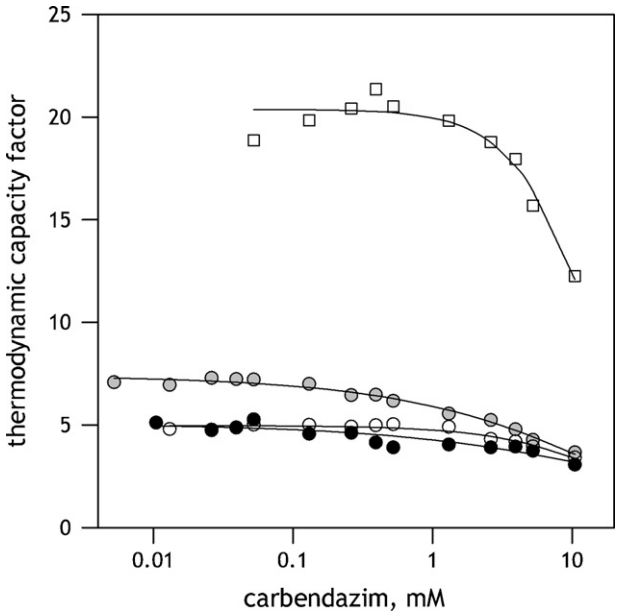

Fig. 5. Thermodynamic capacity factor (m_1 parameter) vs. concentration of injected carbendazim solution for MIP-B (open squares), MIP-S1 (open circles), MIP-S2 (gray circles) and MIP-S3 (black circles).

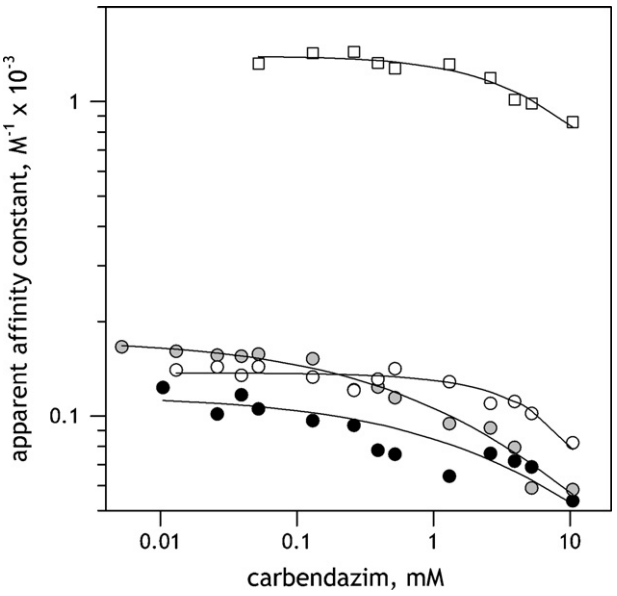

Fig. 6. Apparent affinity constant vs. concentration of injected carbendazim solution for MIP-B (open squares), MIP-S1 (open circles), MIP-S2 (gray circles) and MIP-S3 (black circles).

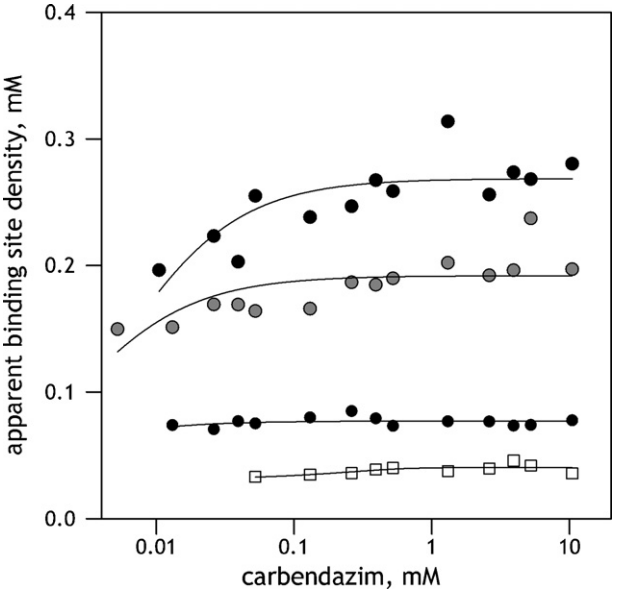

Fig. 7. Apparent binding site density vs. concentration of injected carbendazim solution for MIP-B (open squares), MIP-S1 (open circles), MIP-S2 (gray circles) and MIP-S3 (black circles).

independent of the amount of analyte injected. In Fig. 5, the plots of thermodynamic capacity factor versus the amount of carbendazim introduced into the columns are reported. For all the columns packed with imprinted polymers prepared in silica beads, the decrease of the capacity factor is significant when the amount of analyte injected into the column is bigger than 0.1 mM (corresponding to an injection of about 120 ng of carbendazim), while the bulk polymer shows a significant overloading only for carbendazim concentrations higher than one order of magnitude (about 1 mM), indicating a larger binding capacity for the imprinted polymer prepared by bulk polymerization compared to polymers prepared in silica beads. Moreover, neither the porosity of the starting silica beads nor its surface area seems to condition the binding capacity of the imprinted beads, as the values of the thermodynamic capacity factors measured for the polymers prepared in silica beads show limited differences in relation to the beads porosity and surface area – a difference which is completely suppressed when the columns are overloaded. On the contrary, the type of polymerization process (in bulk or in silica) largely influences the resulting binding properties that reduce when polymerization in silica beads is used instead of bulk polymerization.

In accordance with the NLC model, the binding capacity is proportional to the apparent affinity constant and to the surface area through the binding site density (Eq. (6)). In Fig. 6 the apparent affinity constant is plotted against the amount of carbendazim introduced in the columns. It reveals a large dependence of the numerical values of K from the corresponding carbendazim concentrations, with decreasing values of affinity when the analyte concentration increases. As previously shown by Umpleby et al. [22], this dependence could be explained by the presence in the molecularly imprinted polymers of continuous distributions of binding sites characterized by affinity constants distributed at quite large value intervals, with small populations of high affinity sites and large populations of low affinity sites. Thus, in a column eluted in the presence of very low amounts of carbendazim, the competition between different classes of binding sites is dominated by low density but high affinity sites. In these conditions, peak profiles are principally influenced by these binding sites, with a consequent high value for apparent affinity constants. On the contrary, in the presence of increased amounts of carbendazim, small populations of high affinity binding sites are nearly saturated, and the partition equilibrium is controlled by larger populations of weaker binding sites, which become the principal factor governing the peak profile, determining low values for the apparent affinity constants. It is noteworthy that apparent affinity constants measured for the bulk polymer are significantly higher than affinity constant measured for imprinted polymers prepared in silica beads in the whole range of experimental measurements. Thus, as observed in the case of the thermodynamic capacity factor, the main factor controlling the affinity of an imprinted polymer for the template molecule is not the porosity of the starting silica beads but the type of polymerization, in bulk or in silica.

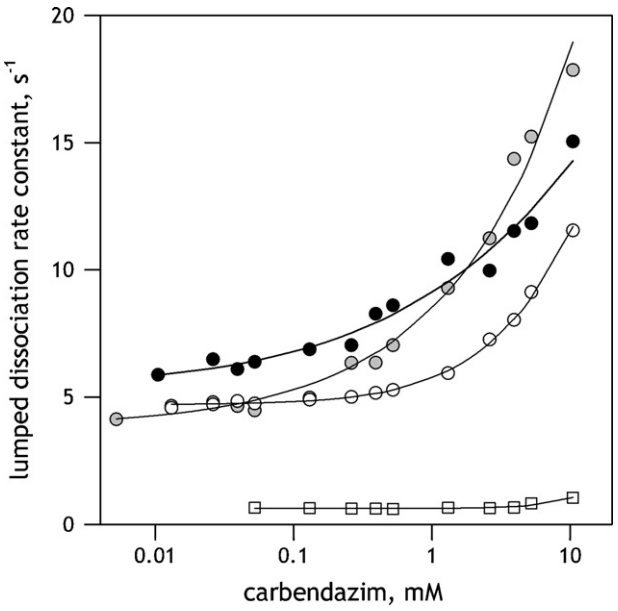

Fig. 8. Lumped dissociation rate constant vs. concentration of injected carbendazim solution for MIP-B (open squares), MIP-S1 (open circles), MIP-S2 (gray circles) and MIP-S3 (black circles).

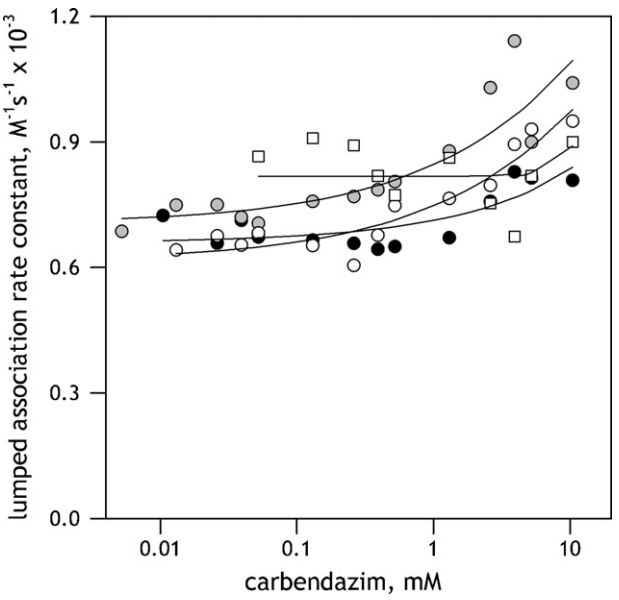

Fig. 9. Lumped association rate constant vs. concentration of injected carbendazim solution for MIP-B (open squares), MIP-S1 (open circles), MIP-S2 (gray circles) and MIP-S3 (black circles).

As regards the apparent binding site density, in Fig. 7 it is plotted against the amount of carbendazim introduced into the columns. The calculated values slightly increase with the amount of carbendazim introduced into the columns. This trend could be explained by the increasing numbers of binding sites (of decreasing affinity) involved in the binding with increasing amounts of carbendazim. More interesting is the fact that the bulk polymer shows the lowest binding site density, while the polymers prepared in silica beads, characterized by nearly comparable apparent affinity constants, show higher and increasing binding site densities proportional to the beads mesoporosities. This could be explained considering that binding site accessibility is controlled by the geometric properties of the mesopores of the beads. As carbendazim has an approximated hydrodynamic diameter of about 1 nm (estimated on the basis of the volume occupied by the solvent-accessible surface measured with a probe of 0.14 nm), in the dynamic process of partition between mobile and stationary phase many mesopores could be accessed only with relative difficulty by this analyte. Thus, the number of binding sites actually available (i.e. the effective density of binding sites) should increase when mean mesopore diameter increases. The low binding site concentration shown by the bulk polymer can be interpreted as the consequence of its very broad pore size distribution (see Fig. 3), where small diameter mesopores are a significant fraction of the resulting total porosity.

The apparent affinity constant defined in accordance with the NLC model can be seen as the ratio between the association and dissociation rate constants. Anyway, this model does not give the rate constant corresponding to the solute–binding site interaction, but it gives rather an apparent – lumped – rate constant resulting from the contribution of many processes operating in the column. In fact, aside from the "true" rate constant, kinetic constants from all the mass transfer processes from the bulk of the mobile phase to the stationary phase should be considered. Thus, it is not surprising that polymers imprinted with the same template, but through different approaches, show completely different lumped rate constants. This is the case for polymers prepared by bulk or in silica polymerization. In Fig. 8 the lumped dissociation rate constants plotted against the amount of carbendazim introduced in the column show a marked difference between the two kinds of polymerization. In fact, as observed in the case of the thermodynamic capacity factors and apparent affinity constants, the main factor controlling the magnitude of the dissociation rate constant is not the porosity of the starting silica beads but the type of polymerization, in bulk or in silica. As the dissociation mechanism should be the same for all the imprinted binding sites, the morphology of the imprinted materials plays a significant role in determining the magnitude of the lumped kinetic constants, which result reduced markedly in the case of the bulk polymer. Contrarily, the experimental values obtained for the lumped association rate constants, reported in Fig. 9, do not show any substantial difference between the polymers prepared in silica beads and the polymer obtained by bulk polymerization. It should be considered anyway, that in not overloading conditions (for carbendazim concentration under 0.1–1 mM) the numerical difference between k_a calculated for all the polymers is quite limited (about a factor of 2), while the same difference measured for k_d is much larger, covering an interval of about 10. Thus it is plausible that different polymer morphologies influence the binding kinetics in different ways, with a larger effect on the dissociation kinetics.

4. Conclusions

The chromatographic evaluation of the binding behaviour of imprinted polymers prepared through two different approaches – by bulk polymerization and by polymerization in silica beads – show that the porosity and surface area of the resulting imprinted materials are related to the corresponding values of the silica beads and quite different in pore diameter distribution compared to the bulk material. Contrarily, when considering silica supports with porosity distributed in the mesopore range, the support porosity seems not to be the main parameter in the fine tuning of the binding properties of the resulting imprinted polymers, as the binding properties of the imprinted beads are strongly affected by the polymerization approach used but not by the initial porosity of the silica beads, with the sole exception of the binding site density, that appears to be inversely proportional to them. Moreover, the values of capacity factors and apparent affinity constants show that the bulk material binds the carbendazim more efficiently than polymers prepared in silica beads.

Acknowledgements

This work was supported by the Italian Ministry of Instruction, University and Research (MIUR project COFIN05 Ref. 2005030782).

References

[1] P.A.G. Cormack, A.Z. Elorza, J. Chromatogr. B 804 (2004) 173.
[2] C.J. Tan, Y.W. Tong, Anal. Bioanal. Chem. 389 (2007) 369.
[3] S. Wei, B. Mizaikoff, J. Sep. Sci. 30 (2007) 1794.
[4] J. Haginaka, J. Chromatogr. B 866 (2008) 3.
[5] E. Yilmaz, K. Haupt, K. Mosbach, Angew. Chem. Int. Ed. Eng. 39 (2000) 2115.
[6] M.M. Titirici, A.J. Hall, B. Sellergren, Chem. Mater. 14 (2002) 21.
[7] M.M. Titirici, A.J. Hall, B. Sellergren, Chem. Mater. 15 (2003) 822.
[8] M.M. Titirici, B. Sellergren, Anal. Bioanal. Chem. 378 (2004) 1913.
[9] W.S. Lee, T. Takeuchi, Anal. Sci. 21 (2005) 1125.
[10] E. Yilmaz, O. Ramström, P. Möller, D. Sanchez, K. Mosbach, J. Mater. Chem. 12 (2002) 1577.
[11] F.G. Tamayo, A. Martin-Esteban, J. Chromatogr. A 1098 (2005) 116.
[12] F.G. Tamayo, M.M. Titirici, A. Martin-Esteban, B. Sellergren, Anal. Chim. Acta 542 (2005) 38.
[13] L. Anfossi, C. Baggiani, P. Baravalle, C. Giovannoli, L. Guzzella, F. Pozzoni, Anal. Lett. 42 (2009) 807.
[14] K.S.W. Sing, Pure Appl. Chem. 54 (1982) 2201.
[15] J.L. Wade, A.F. Bergold, P.W. Carr, Anal. Chem. 59 (1987) 1286.
[16] C. Baggiani, P. Baravalle, L. Anfossi, C. Tozzi, Anal. Chim. Acta 542 (2005) 125.
[17] P. Sajonz, M. Kele, G.M. Zhong, B. Sellergren, G. Guiochon, J. Chromatogr. A 810 (1998) 1.
[18] P. Szabelski, K. Kaczmarski, A. Cavazzini, Y.B. Chen, B. Sellergren, G. Guiochon, J. Chromatogr. A 964 (2002) 99.
[19] H. Kim, G. Guiochon, J. Chromatogr. A 1097 (2005) 84.
[20] B. Toth, K. Laszlo, G. Horvai, J. Chromatogr. A 1100 (2005) 60.
[21] B. Toth, T. Pap, V. Horvath, G. Horvai, J. Chromatogr. A 1119 (2006) 29.
[22] R.J. Umpleby, S.C. Baxter, A.M. Rampey, G.T. Rushton, Y.Z. Chen, K.D. Shimizu, J. Chromatogr. B 804 (2004) 141.